Tensile Stress in Human Ribs throughout the Lifespan

Amanda M. Agnew[1], Kevin Moorhouse[2], Michelle Murach[1], Susan E. White[3], Yun-Seok Kang[1]

Abstract The purpose of this study is to characterize the tensile stress of human ribs across the lifespan. One-hundred six whole ribs from 43 subjects were experimentally tested in a bending scenario using a custom fixture to simulate a dynamic frontal impact. Ages ranged from nine to 92 years old, with a mean age of 60 years and representation in each decade. Strain gauges on each rib were used to determine time of failure. Post-impact, a section adjacent to the fracture site was used for precise calculations of geometric properties. Tensile stress due to bending was determined at the time of fracture for each rib, and results indicate a significant decline in stress with increasing age. This research may be particularly useful for application in the construction of finite element models. Rib material properties in the context of structural response as presented here can aid with advancing knowledge about age-related changes in the rib as well as having implications for better understanding of whole thorax response and injury.

Keywords elderly, fracture, pediatric, rib, strength

I. INTRODUCTION

The thorax is an important region for biomechanical studies because it is often injured in motor vehicle crashes [1]. Rib fractures are one of the most common injuries in the elderly, especially in motor vehicle crashes, and these injuries can greatly affect morbidity, mortality and quality of life in elderly individuals [2]. Rib fractures in children are no less important. However, few studies exist that explore the mechanical properties and behavior within immature human bone specimens [3-4] which are necessary to help understand injury mechanisms in children. Traumatic injury from motor vehicle crashes is a major cause of death in children [5] and the mechanisms of injury require further investigation.

Assigning accurate and precise material properties to bone when constructing computational models can be important to maximize a realistic response of the model in an impact scenario and predict fracture timing and location [6-7]. Currently, it is difficult to create age-specific models of the thorax and ribs because 1) pediatric and young adult material property data are rare, and 2) the amount of material property variation across the population is unknown. Many researchers have evaluated rib properties through experimental testing [7-9] but no study exists that includes an age-comprehensive dataset tested under the same repeatable loading conditions. The goal of this study is to identify trends in rib

A.M. Agnew, PhD, is an assistant professor of Anatomy at The Ohio State University, Columbus, OH, USA (tel: +1 614 366 2005, fax: +1 614 292 7659, email: amanda.agnew@osumc.edu). Author affiliations: [1]Injury Biomechanics Research Center (IBRC), The Ohio State University; [2]National Highway Traffic Safety Administration (NHTSA), Vehicle Research & Test Center (VRTC); [3]Division of Health Information Management and Systems, The Ohio State University.

tensile stress at fracture from early childhood through old age in a large sample to capture population variation. It is expected that age-related trends in tensile stress will specifically reveal a decrease in stress with increasing age.

II. METHODS

Sample

One-hundred six ribs were obtained from 43 post-mortem human subjects (PMHS) through the Division of Anatomy's Body Donation Program at The Ohio State University and Lifeline of Ohio. All ethics review requirements were met for this research. Only middle ribs (anatomical levels 3-8) were included in the sample to maintain morphological similarity. Complete ribs, from the head to the costo-chondral joint, were excised post-mortem, wrapped in saline-soaked gauze and frozen at -20^{o}C until the time of testing. Subjects included in the sample are of both sexes and range in age from 9 to 92 years old. The mean BMI for the sample was 24.1 (SD = 5.4) and most subjects were considered to be either 'normal' (18.5-24.9) or 'overweight' (25-29.9). See Table 1 for a summary of subject demographics. The only exclusion criterion employed was previously documented thoracic trauma. Otherwise, ribs from any individual were accepted into the study, since a goal of this study is to capture the amount of variation present in the population.

Ribs were thawed and cleaned of all excess external soft tissue (e.g., muscles, ligaments) prior to testing. The vertebral and sternal ends were then potted in 4x4x3 cm^3 blocks of Bondo® Body Filler (Bondo Corporation, Atlanta, GA). During potting, a ratio of hardener to base was used such that the exothermic reaction of the Bondo® was controlled to not exceed 37.7^{o}C (i.e., approximate body temperature). In this way, the rib did not experience any extreme heat that could cause damage and potentially affect the bone properties. Ribs were oriented in the pots in a single plane to reduce torsional effects during the event. Four strain gauges (Vishay Micro-Measurement, Shelton, CT, CEA-06-062UW-350) were adhered to each rib and were used to determine fracture timing. Gauges were adhered on the pleural surface at 30% and 60% of the curve length from the vertebral end of the potted rib, and two more were adhered at corresponding locations on the cutaneous surface (see Fig. 1).

Ribs were allowed to reach room temperature (~21^{o}C) prior to testing. The specimens remained hydrated throughout the testing process by leaving them wrapped in saline-soaked gauze whenever possible and spraying them continually with fresh saline. This rigor was necessary since proper hydration is needed to measure realistic bone properties [10].

Table 1
Subject demographics

Subject ID	Sex	Age (yrs)	BMI* (kg/m^2)	n
XL418	M	9	21.1	3
L0100	F	10	15.1	1
L0216	M	20	25.1	4
A6233	M	21	22.6	6
A6248	M	26	17.6	3

L0214	M	27	28.4	2
A6141	M	29	25.6	5
L0132	M	30	24.6	1
L0032	M	30	25.9	1
L0213	M	39	27.4	1
A6565	M	40	20.0	1
A6134	M	42	25.2	2
L0108	M	42	32.0	2
L0252	M	42	24.3	1
L0221	M	43	36.1	2
A6669	M	47	12.7	1
L0247	M	48	36.7	3
L0004	M	51	22.2	1
A6504	M	52	25.3	1
A6327	F	64	19.0	1
A6169	M	67	30.4	6
A6236	M	69	21.9	2
A5998	M	71	20.9	5
A5730	M	73	21.5	1
A6172	M	75	25.4	5
A6462	F	75	17.7	1
VSM85	M	76	28.1	1
A6090	F	77	27.8	3
A6035	M	79	22.2	6
A6444	M	79	35.2	2
A6034	F	80	26.4	2
A6063	M	82	24.5	2
A6367	M	84	26.5	5
A6283	M	85	12.5	1
A6583	M	85	22.7	3
A6390	M	86	16.3	4
A6024	M	87	27.5	4
A6011	M	88	22.8	3
A6652	F	88	19.8	2
A6281	F	90	21.8	1
A6369	F	90	29.0	2
A5894	F	92	24.5	1
A6591	F	92	24.7	2
N = 43	10 F 33 M	Mean = 60 years	Mean = 24.1	n = 106 ribs

*BMI (body mass index) = weight/stature^2, N = number of subjects, n= number of ribs tested

Data Collection

A custom pendulum fixture was constructed based on the concept introduced by [11] and modified by [12] to load whole ribs horizontally (Fig. 1). The mass of the pendulum impactor is 54.4 kg. Each end of the fixture is separated to minimize vibration effects. The two ends of the potted rib were secured firmly in rotating cups with screws to each portion of the fixture. These cups allow for freely rotating pivot joints at each rib end. A rotary potentiometer (14CB1, Servo Instrument Corportation, Baraboo, WI) was incorporated at each of these joints to measure rotation during the event. A 6-axis load cell (CRABI neck load cell, IF-954, Humanetics, Plymouth, MI) was situated behind the stationary plate and was positioned to align with the center of the vertebral rib-end pot. The stroke of the moving plate was controlled according to the span length of each rib to create a consistent test condition with varying rib sizes.

A linear displacement string-potentiometer (Rayelco P-20A, AMETEK, Inc. Berwyn, PA) was attached to the moving plate to measure the displacement of the sternal end of the rib (comparable to anterior-posterior compression of the thorax in a whole-body test scenario). An accelerometer (Endevco 7264G-2K, San Juan Capistrano, CA) was also attached to the moving plate to measure acceleration and calculate velocity of the moving plate. These test conditions are meant to simulate a dynamic frontal impact in a simplified scenario. All impacts occurred between 1.0 m/s and 2.0 m/s, and the primary loading axis was defined as the x-axis according to the SAE J211 coordinate system (Fig. 1). High-speed video was recorded at 1000 fps to track black markers on the surface of the rib during the event. TEMA motion software (Image Systems Motion Analysis, Linköping, Sweden) was used to determine local displacements (X and Y directions) at the point closest to fracture.

After impact, a segment of the rib (~15 mm) adjacent to the fracture location was removed, gently macerated, and embedded in methylmethacrylate. From the resulting block, a thin section (~70 microns) closest to the fracture was cut using a Diamond Wire Histo Saw (Model 3241, DDK, Inc. Wilmington, DE) and mounted on a microscopic glass slide with Eukitt mounting medium. Cross-sectional images at 40x magnification (resolution = 909 p/mm) were acquired using cellSens Dimension imaging software with an Olympus BX63 microscope equipped with an Olympus DP73 high-resolution camera. Cortical boundaries (periosteal and endosteal) were manually traced by a researcher experienced in skeletal histomorphometry (AMA) to determine Cortical Area (Ct.Ar) in cellSens. The isolated-cortex image was then imported into ImageJ (NIH) to allow the MomentMacro plug-in [13] to calculate cortex-specific section modulus (Zx).

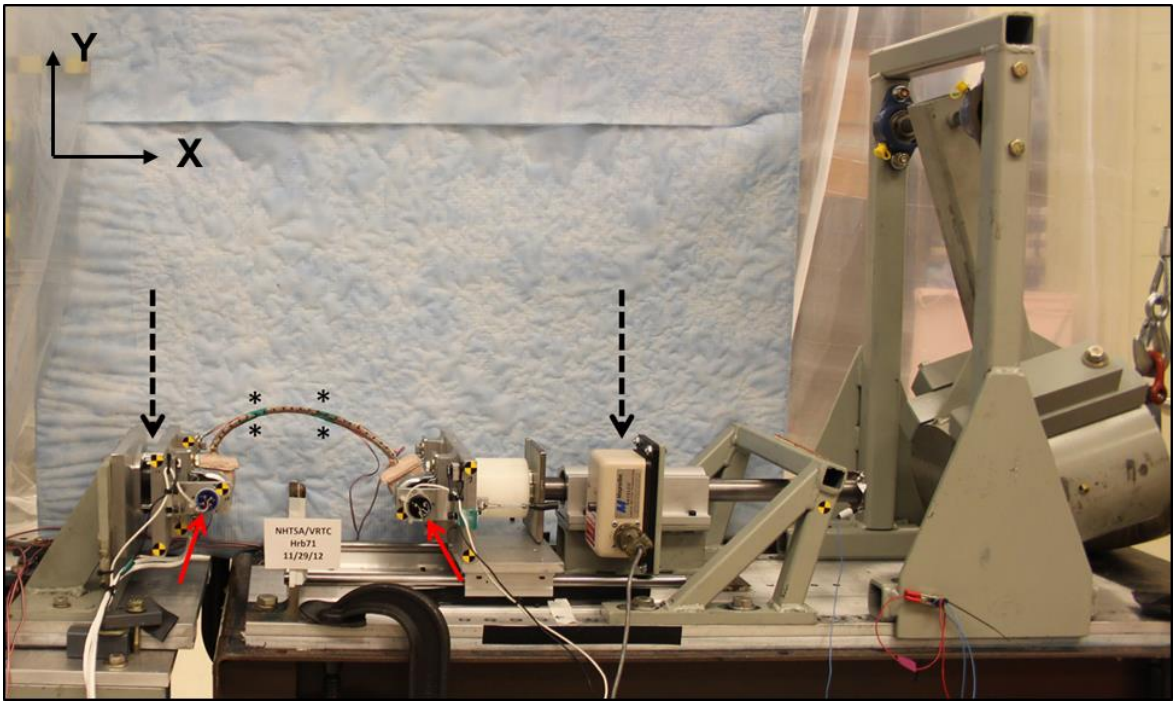

Figure 1. Experimental test set-up. The pendulum impactor is on the right side of the image. Asterisks (*) represent the location of strain gauges on the rib. Left and right dashed arrows (black) show the location of the 6-axis load cell and displacement pot, respectively. Solid arrows (red) show the rotary potentiometers. The stationary end of the fixture (left) holds the vertebral rib end, while the moving end (right) holds the sternal end (i.e., a frontal impact scenario).

Data Analysis

Load cell, accelerometer and linear potentiometer data were filtered at 300 Hz using CFC 180. In order to calculate stress at the time and location of fracture, combined loads (i.e., compressive force and bending moment) were first determined. To determine the compressive force at the fracture locations, global force data from the load cell in the X and Y directions were transformed using a transformation matrix to a local coordinate system. Rotation angle was determined from the high-speed video frame just prior to fracture. The angle between the local coordinate system and the global coordinate system was measured using ImageJ software. The x axis of the local coordinate system corresponds to the neutral axis (NA) of the rib at the cross section where fracture occurred (Fig. 2). In order to calculate bending moment (M) at fracture locations, forces in the X and Y directions measured from the load cell were multiplied by the vertical and horizontal distances, respectively, between the load cell and marker closest to fracture obtained from the TEMA analysis. Cross-sectional properties (Ct.Ar and Zx), the transformed compressive force (Fx) and the bending moment (M) at the fracture location were then used to determine the tensile stress described in Eq (1).

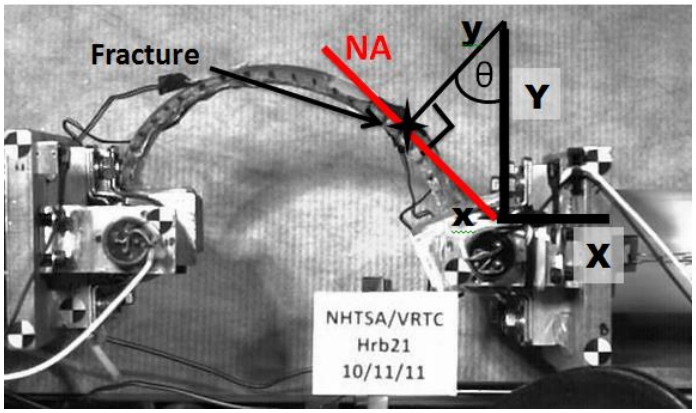

Figure 2. Image of rib set-up showing global (X, Y) and local (x, y) coordinate systems

$$\sigma = -\frac{Fx}{Ct.Ar} \pm \frac{M}{Zx} \quad (1)$$

where σ : stress at time of fracture (MPa)
Fx : transformed axial force (N)
M : bending moment at fracture location (N-mm)
Ct.Ar : cross sectional cortical area (mm^2)
Zx : section modulus (mm^3)

A multi-level model was used to assess the effect of age on tensile stress. The intraclass correlation in stress that occurs between subjects is 0.61, meaning 39% can be attributed to intra-individual variation. Although there is more variation between subjects than within subjects, the non-independence of data points suggests a traditional regression model is inappropriate. Therefore, the multi-level model was used so that the correlation between ribs from the same subjects could be reflected in the model. In multi-level modeling, the level 1 model allows the average stress per subject (intercept term) to be represented by a random effect. The level 2 model allows inclusion of a subject-level effect of age. The model was fit using Proc Mixed with restricted maximum likelihood estimation in SAS 9.3. An unstructured variance covariance matrix was assumed since there was no prior knowledge of the relationship between the stress values of various ribs within each subject.

III. RESULTS

Table 2 displays summary descriptive statistics for tensile stress at the time of fracture for each subject. The arithmetic mean tensile stress for the entire sample is 175.48 (SE = 16.62) MPa. The model indicates that the fixed effect for age on tensile stress is significant ((df = 63) = -4.40, $p < 0.0001$), as shown in Table 3. The amount of variance explained by age is estimated using a pseudo R^2 calculation [14], a measure of how much of the between-subject variance is explained by the variable (not how much of the total variance in stress is explained, as a normal R^2 would). Age explains 40.4% (pseudo R^2) of the variance that is attributed to the subject level stress values as is shown in Figure 3. The estimate of the average stress is 175.26 based on the model presented in Table 3. This estimate reflects the dependent nature of the data since multiple ribs were tested from the same subjects. The model provides an estimate of -1.25 (SE = 0.28) as the amount of change in stress for each year of increased subject age.

Table 2
Descriptive statistics per subject

Subject ID	Age (yrs)	Mean Tensile Stress (MPa)	SE Mean
XL418	9	163.0	51.5
L0100	10	147.87	*
L0216	20	162.6	15.2
A6233	21	267.3	24.9
A6248	26	244.04	5.2
L0214	27	189.1	20.9
A6141	29	301.4	21.9
L0132	30	192.06	*
L0032	30	233.28	*
L0213	39	261.35	*
A6565	40	226.93	*
A6134	42	280.97	5.79
L0108	42	237.89	8.41
L0252	42	246.54	*
L0221	43	206.3	19.3
A6669	47	169.94	*
L0247	48	181.5	21.5
L0004	51	142.22	*
A6504	52	152.04	*
A6327	64	191.23	*
A6169	67	145.5	14.8
A6236	69	98.5	25.0
A5998	71	172.6	28.0

A5730	73	174.2	*
A6172	75	156.6	16.4
A6462	75	150.9	*
VSM85	76	237.46	*
A6090	77	157.4	12.0
A6035	79	135.6	13.2
A6444	79	121.5	22.0
A6034	80	160.27	6.66
A6063	82	197.9	10.4
A6367	84	143.93	4.68
A6283	85	120.53	*
A6583	85	148.2	6.71
A6390	86	99.9	13.5
A6024	87	65.2	10.9
A6011	88	142.4	15.4
A6652	88	216.4	18.3
A6281	90	111.99	*
A6369	90	97.2	19.5
A5894	92	80.25	*
A6591	92	213.7	54.8
Mean	**60 years**	**175.26**[a]	**16.62**

Asterisk (*) indicates that a SE mean could not be calculated because only one rib was tested for that subject.
[a]average stress was calculated using the following formula based on the model results of the estimate of the intercept and age and the mean age of 60 years as shown in Table 3: 250.14 – 1.248 * 60 = 175.26.

Table 3
Solution for age effects on tensile stress

Effect	Estimate	Standard Error	DF	t-value	p-value
Intercept	250.14	18.6171	41	13.44	<0.0001
Age	-1.2480	0.2837	63	-4.40	<0.0001

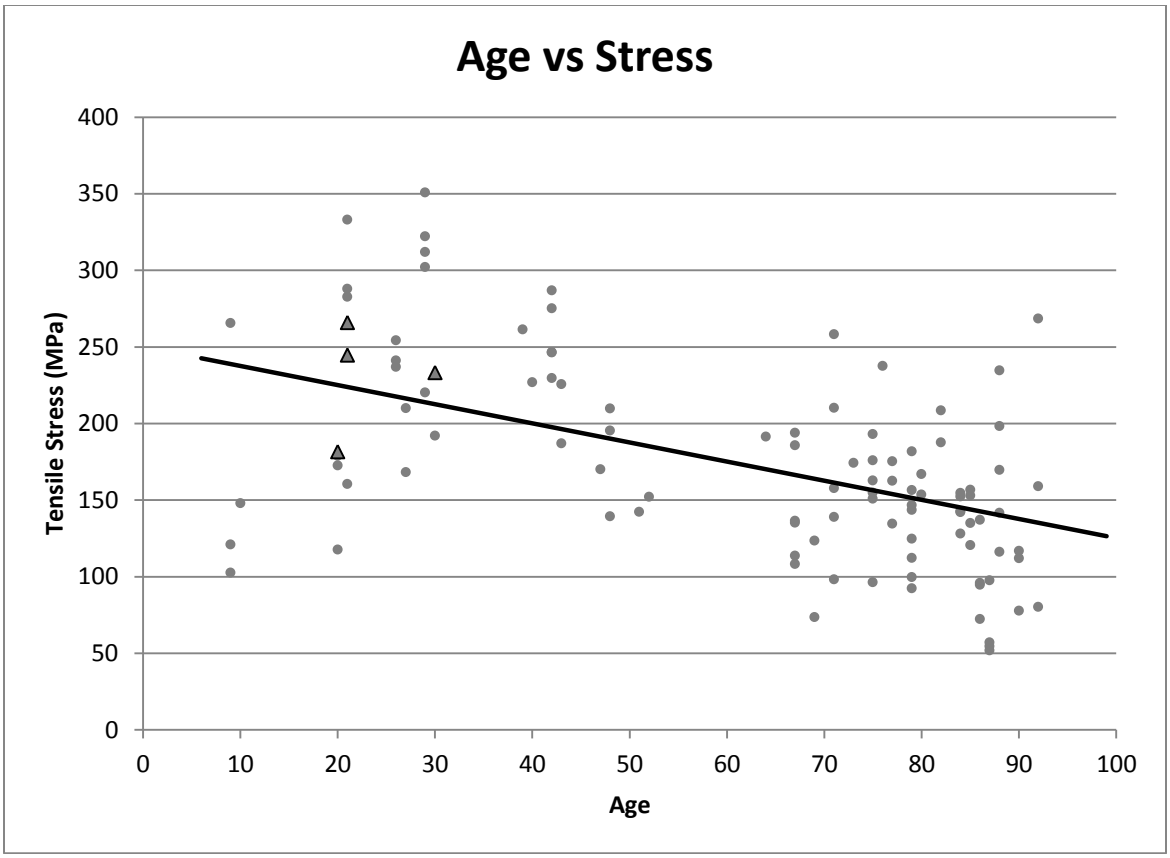

Figure 3. Scatterplot showing the relationship between age and tensile stress for all ribs tested (n=106). The line represents an implied marginal model based on the fixed effects estimate (an "average" regression for subjects). Four ribs in the sample did not fail, so stress was calculated at the time of peak strain instead of at the time of fracture. These data points are denoted with triangles, instead of circles.

IV. DISCUSSION

The results of this study indicate an inverse relationship between age and tensile stress at the time of fracture due to bending in ribs dynamically loaded to failure. Similarly, other studies have also shown ultimate stress to decrease with age in mechanical tests on human long bones [15-16], although it is difficult to find rib-specific datasets for comparison that incorporate similarly broad age ranges. Stein and Granik [17] performed quasi-static rib segment 3-point bending on a large sample of males from young adulthood to elderly years. A significant relationship between age and ultimate stress was discovered (stress decreased significantly with advanced aging). However, the mean stress value (106.2 MPa) is difficult to compare to the current study since testing was performed at quasi-static loading rates.

A few studies exist which have tested rib specimens at dynamic rates. Kemper et al. [18] subjected 117 cutaneous coupons from all ribs from subjects aged 18-67 to tensile loading and found a mean ultimate stress of 124.2 MPa with no relationship between stress and age. In a similar approach, tests of coupons from ribs 4-7 from six different subjects (ages 42-81 years) resulted in a mean ultimate stress of 130.9 MPa, and again no relationship between stress and age was found [8]. Stitzel et al. [7] subjected

cutaneous coupons to dynamic 3-point bending and found a corrected[1] mean ultimate stress of 136 MPa, which converts to 212.2 MPa when not considering plasticity. This unadjusted mean stress (212.2 MPa) is high compared to other published mean rib stress values, but is probably more appropriate since elderly bone is less likely to exhibit any plastic response to loading (it is more brittle). They could not explore age effects because all four subjects were elderly. A significant amount of stress values in the current study fall above 200 MPa from subjects ranging in age from 20-92 years (Fig. 3). All other previous studies report considerably lower mean ultimate stress values and this is likely due to an age bias in samples, as well as small sample sizes. These differences in mean values and approaches highlight the importance of utilizing a large sample size and understanding the full range of variation possible.

Pediatric specimens in the current study include a 9 and 10 year old. The mean tensile stress at fracture of the four ribs from these two individuals is 159.18 MPa. If considering specimens from a similarly aged individual (9 year old) in a previous study in which quasi-static 3-point bending was applied, the mean ultimate stress reported for four ribs from this individual was 119.6 MPa [20]. Differences in stress values between these studies are not surprising based on the varied loading rates (quasi-static versus dynamic) and boundary conditions.

The implied marginal model estimated here shows a decrease in tensile stress with age, but assumes a linear relationship between the variables. However, it is likely that the true relationship between stress and age is non-linear in nature. A potential trend is apparent upon visual inspection where a peak is reached in the young adult years (Figure 3). Forman et al.'s study [3] found factors representing the ultimate stress of femoral bones to have a slight relationship with age, where values remained fairly constant until around age 40, after which a subtle decline was noted. A similar trend has also been observed for rib structural properties with age [21]. This apparent non-linear relationship will be explored further in future work that includes more data points in the younger age range (i.e., sub-adults).

A few limitations must be addressed for this study. Not all ages are represented equally across the sample and more males are included than females. Future work will aim to even out the sample by testing ribs from more subjects. Also, the effects of rib level were not explored in this study. This omission was deliberate as many studies have reported no differences in intrinsic properties between rib levels [8-9, 17-18] and investigation of this was not a goal of the study.

Tensile stress was calculated from a structural test. It has been suggested in past rib work that linear elastic beam equations will overestimate ultimate stress values because they do not take into account the plasticity of the rib [8]. Our reported stress values include elastic and plastic components. Other papers attempting to model rib stress have modeled only the elastic response with a correction factor [7]. Results may not match between actual and theoretical stress and should be approached with caution.

Since the estimate of residual covariance is significant ($p < 0.001$), there is still a significant amount of variance to be explained by subject-level variables other than age. In fact, the level I model showed that while approximately 61% of variance is between subjects, the remaining 39% is within subjects. Future work will include a quantification of the degree of remodeling and associated intracortical porosity as well as the accumulation of microcracks to attempt to understand why the rib displays the range of stress values seen here. Other studies have shown a relationship between age and ultimate stress in long bones and suggest it can be explained by bone microstructure [22-24], so including such variables in the multi-level model as rib-level covariates may explain more of the variation observed in rib stress within subjects.

[1] Considers plasticity and is adjusted according to [13] and [19]

Previous efforts have been made to develop finite element thorax models that can provide biomechanical responses and predict injuries [11, 25-26]. The results from the current study can be used to provide a more accurate correction factor based on how actual cross-sectional characteristics and the relationship between ultimate stress and tensile fracture stress change with age or identify fracture mechanisms or location in existing models. Unlike coupon tests, this study explored responses of intact rib structures in a bending mode that more realistically reflects full ribcage deformations, which can be used to investigate injury tolerance of the ribs as a function of age with respect to both material properties and geometry (and more realistically as part of the thorax). It is promising that the same trend of decreased rib stress with age found here is consistent with an observed increase in thoracic region injury severity with age seen in whole body studies [27].

V. CONCLUSIONS

In summary, tensile stress at the time of fracture due to bending in human ribs was found to significantly decrease with advancing age. More work is underway to understand mechanisms for failure and the sources of variation within and between subjects outside of age effects. Accurate material properties have a significant effect on the efficiency and outcome of computational models [28]. Characterizing the degree of variation in ultimate stress between and within subjects with age will expand the utility of finite element model creation. Ultimately, a more precise approach to modeling using age-specific rib properties will assist in defining injury mechanisms and criteria for rib fractures as well as for the entire thorax [7].

VI. ACKNOWLEDGEMENTS

This research would not be possible without the selfless gifts that the donors and their families have shared, and it is only through their donations that progress is made in saving the lives of others. Donations were made through the Body Donation Program at The Ohio State University and Lifeline of Ohio, and were graciously collected with the help of the staff at both places. Thank you to NHTSA for sponsoring this research, and especially Bruce Donnelly and Jason Stammen for their continued support. The Transportation Research Center, Inc., especially Rod Herriott and Patrick Brown, contributed as well. IBRC associates and students to thank include: John H Bolte IV, Julie Bing, Kyle Icke, Rakshit Ramachandra, Michelle Schafman, Tim Gocha, Victoria Dominguez, Randee Hunter, Alex Redrow and Matt Reynolds.

VII. REFERENCES

[1] Kent R, Henary B, Matsuoka F. On the fatal crash experience of older drivers. *49th Annual Proceedings, Association for the Advancement of Automotive Medicine*, 2005.

[2] Kent R, Woods W, Bostrom O. Fatality risk and the presence of rib fractures. *Annals of Advances in Automotive Medicine,* 2008, 52:73-84.

[3] Forman J, de Dios E, et al. 2012. Fracture tolerance related to skeletal development and aging throughout life: 3-point bending of human femurs. *Proceedings of IRCOBI Conference*, 2012, pp. 524-539, Dublin, Ireland.

[4] Sturtz G. Biomechanical data of children. *Stapp Car Crash Conference,* 1980*,* 24:511-549.

[5] NHTSA. Children. Traffic Safety Facts DOT HS 811 387, 2009.

[6] Li Z, Kindig MW, Subit D, Kent R. Influence of mesh density, cortical thickness and material properties on human rib fracture prediction. *Medical Engineering and Physics,* 2010*,* 32(9):998-1008.
[7] Stitzel J, Cormier JM, et al. Defining regional variation in the material properties of human rib cortical bone and its effect on fracture prediction. *Stapp Car Crash Journal,* 2003, 47:243-265.
[8] Kemper A, McNally C, Pullins C, Freeman L, Duma SM, Rouhana S. The biomechanics of human ribs: Material and structural properties from dynamic tension and bending tests. *Stapp Car Crash Journal,* 2007, 51:1-39.
[9] Yoganandan N, Pintar F. Biomechanics of human thoracic ribs. *Journal of Biomechanical Engineering,* 1998, 120:100-104.
[10] Reilly D, Burstein A, Frankel V. The elastic modulus for bone. *Journal of Biomechanics*, 1974, 7:271 275.
[11] Charpail E, Trosseille X, Petit P, Laporte S, Lavaste F, Vallencien G. Characterization of PMHS ribs: A new test methodology. *Stapp Car Crash Journal*, 2005, 49:183-198.
[12] Kindig MW. Tolerance to failure and geometric influences on the stiffness of human ribs under anterior-posterior loading: University of Virginia, 2010.
[13] Ruff C. no date. MomentMacroJ program. [internet]: Available at: http://www.hopkinsmedicine.org/fae/mmacro.htm.
[14] Xu R. Measuring explained variation in linear mixed effects models. *Stat Med*, 2003, 22:3527-3541.
[15] Burstein A, Reilly D, Martens M. Aging of bone tissue: mechanical properties. *Journal of Bone and Joint Surgery*, 1976, 58A:82-86.
[16] Lindahl O, Lindgren A. Cortical bone in man. 2. Variation in tensile strength with age and sex. *Acta Orthopaedica Scandinavica*, 1967, 38:141-147.
[17] Stein ID, Granik G. Rib structure and bending strength: An autopsy study. *Calcified Tissue Research,* 1976, 20(1):61-73.
[18] Kemper A, McNally C, et al. Material properties of human rib cortical bone from dynamic tension coupon testing. *Stapp Car Crash Journal*, 2005, 49:199-230.
[19] Burstein A, Currey J, Frankel V, Reilly D. The ultimate properties of bone tissue: The effects of yielding. *Journal of Biomechanics*, 1972, 5:35-44.
[20] Agnew A, Moorhouse K, et al. The response of pediatric ribs to quasi-static loading: Mechanical properties and microstructure. *Annals of Biomedical Engineering*, 2013, 41(12):2501-2514.
[21] Agnew A, Moorhouse K, Kang Y, Herriott R, Bolte J. 2013b. Age-related changes in stiffness in human ribs. *Proceedings of IRCOBI Conference,* 2013, Gothenburg, Sweden.
[22] Evans F. Mechanical properties and histology of cortical bone from younger and older men. *Anat Rec*, 1975, 185:1-12.
[23] McCalden RW, McGeough JA, Barker M, Court-Brown CM. Age related changes in the tensile properties of cortical bone: The relative importance of changes in porosity, mineralization, and microstructure. *Journal of Bone and Joint Surgery*, 1993, 75(8):1193-1205.
[24] Zioupos P, Currey J. 1998. Changes in the stiffness, strength, and toughness of human cortical bone with age. *Bone,* 1998, 20(1):57-66.
[25] Kimpara H, Lee J, et al. Development of a three-dimensional finite element chest model for the 5th percentile female. *Stapp Car Crash Journal*, 2005, 49:251-269.
[26] Li Z, Kindig MW, et al. Rib fractures under anterior-posterior dynamic loads: experimental and finite-element study. *Journal of Biomechanics*, 2010, 43(2):228-234.
[27] Kent R, Lee S, et al. Structural and material changes in the aging thorax and their role in crash protection for older occupants. *Stapp Car Crash Conference Proceedings*, 2005, 49:231-249.
[28] Crandall J, Forman J, et al. Human surrogates for injury biomechanics research. *Clinical Anatomy*, 2011, 24(3):362-371.